Mineralogical Magazine, October 2015, Vol. 79(5), pp. 1175–1184

Flurlite, $Zn_3Mn^{2+}Fe^{3+}(PO_4)_3(OH)_2{\cdot}9H_2O$, a new mineral from the Hagendorf Süd pegmatite, Bavaria, with a schoonerite-related structure

I. E. Grey[1,*], E. Keck[2], W. G. Mumme[1], A. Pring[3], C. M. MacRae[1], R. W. Gable[4] and J. R. Price[5]

[1] CSIRO Mineral Resources, Private Bag 10, Clayton South, Victoria 3169, Australia
[2] Algunderweg 3, D-92694 Etzenricht, Germany
[3] Department of Mineralogy, South Australian Museum, North Terrace, Adelaide, South Australia 5000, Australia
[4] School of Chemistry, University of Melbourne, Parkville, Victoria 3010, Australia
[5] Australian Synchrotron, 800 Blackburn Road, Clayton, Victoria 3168, Australia

[*Received 23 November 2014; Accepted 5 February 2015; Associate Editor: I. Graham*]

ABSTRACT

Flurlite, ideally $Zn_3Mn^{2+}Fe^{3+}(PO_4)_3(OH)_2{\cdot}9H_2O$, is a new mineral from the Hagendorf-Süd pegmatite, Hagendorf, Oberpfalz, Bavaria, Germany. Flurlite occurs as ultrathin (<1 μm) translucent platelets that form characteristic twisted accordion-like aggregates. The colour varies from bright orange red to dark maroon red. Cleavage is perfect parallel to (001). The mineral occurs on mitridatite and is closely associated with plimerite. Other associated minerals are beraunite, schoonerite, parascholzite, robertsite and altered phosphophyllite. The calculated density of flurlite is 2.84 g cm^{-3}. It is optically biaxial (–), $\alpha = 1.60(1)$, $\beta = 1.65(1)$ and $\gamma = 1.68(1)$, with weak dispersion and parallel extinction, $X \approx c$, $Y \approx a$, $Z \approx b$. Pleochroism is weak, with colours: X = pale yellow, Y = pale orange, Z = orange brown. Electron microprobe analyses (average of seven) with FeO and Fe_2O_3 apportioned and H_2O calculated on structural grounds, gave ZnO 25.4, MnO 5.28, MgO 0.52, FeO 7.40, Fe_2O_3 10.3, P_2O_5 27.2, H_2O 23.1, total 99.2 wt.%. The empirical formula, based on 3 P a.p.f.u. is $Zn_{2.5}Mn^{2+}_{0.6}Fe^{2+}_{0.8}Mg_{0.1}Fe^{3+}(PO_4)_3(OH)_2{\cdot}9H_2O$. Flurlite is monoclinic, $P2_1/m$, with the unit-cell parameters (at 100 K) of $a = 6.3710(13)$, $b = 11.020(2)$, $c = 13.016(3)$ Å, $\beta = 99.34(3)°$. The strongest lines in the X-ray powder diffraction pattern are [d_{obs} in Å(I) (*hkl*)] 12.900(100)(001); 8.375(10)(011); 6.072(14)($\bar{1}01$); 5.567(8)(012); 4.297(21)(003); 2.763(35)(040). Flurlite ($R_1 = 0.057$ for 995 $F > 4\sigma(F)$) has a heteropolyhedral layer structure, with layers parallel to (001) and with water molecules packing between the layers. The slab-like layers contain two types of polyhedral chains running parallel to [100]: (*a*) chains of edge-sharing octahedra containing predominantly Zn and (*b*) chains in which Fe^{3+}-centred octahedra share their apices with dimers comprising Zn-centred trigonal bipyramids sharing an edge with PO_4 tetrahedra. The two types of chains are interconnected by corner-sharing along [010]. A second type of PO_4 tetrahedron connects the chains to $MnO_2(H_2O)_4$ octahedra along [010] to complete the structure of the (001) slabs. Flurlite has the same stoichiometry as schoonerite, but with dominant Zn rather than Fe^{2+} in the edge-shared chains. Schoonerite has a similar heteropolyhedral layer structure with the same layer dimensions 6.4 × 11.1 Å. The different symmetry (orthorhombic, *Pmab*) for schoonerite reflects a different topology of the layers.

Keywords: new mineral, Hagendorf Süd pegmatite, flurlite.

Introduction

The phosphate-rich granite pegmatite of Hagendorf-Süd in Bavaria ranks with the Palermo (New Hampshire), Ivigtut (Greenland), Kobokobo

* E-mail: Ian.Grey@csiro.au
DOI: 10.1180/minmag.2015.079.5.11

(DRC) and Tip Top (South Dakota) localities as one of the most mineral-rich granite pegmatites in terms of both the number of new minerals (13) and number of valid minerals found (~170) (Bernard and Hyršl, 2004). Access to the pegmatite minerals at Hagendorf-Süd was made possible when mining for feldspar commenced at the end of the 19th century and a 30 m deep opencut mine was established. Early descriptions of minerals from Hagendorf include publications by Laubmann and Steinmetz (1920) and Müllbauer (1925). It was not until shafts were sunk deep into the body intercepting phosphate-rich zones that new mineral species began to be described. During the 1950s, when triphylite from the albite-phosphate zone was being mined for lithium, no fewer than five new phosphate minerals were characterized as minerals first described from Hagendorf-Süd: scholzite, $CaZn_2(PO_4)_2{\cdot}2H_2O$ (Strunz, 1950); hagendorfite, $(Na,Ca,Mn)_2Mn(Fe^{2+},Fe^{3+})_2(PO_4)_3$ (Strunz, 1954*a*); laueite, $MnFe_2(PO_4)_2(OH)_2{\cdot}\ 8H_2O$ (Strunz, 1954*b*); pseudolaueite, $MnFe_2(PO_4)_2(OH)_2{\cdot}7H_2O$ (Strunz, 1956) and strunzite, $MnFe_2(PO_4)_2(OH)_2{\cdot}6H_2O$ (Frondel, 1958).

The mine was closed and flooded in 1984, preventing further mineral collecting from the pegmatite after this date. Fortunately, large private collections, including one amassed over a period of 30 years by one of us (E.K.) have continued to provide specimens for study. Two new minerals have been characterized recently from specimens in the Keck collection: nordgauite, $MnAl_2(PO_4)_2(F,OH)_2{\cdot}5H_2O$ (Birch *et al.*, 2011) and whiteite-(CaMnMn), ideally $CaMnMn_2Al_2(PO_4)_4(OH)_2{\cdot}8H_2O$ (Yakovenchuk *et al.*, 2012). The new mineral, flurlite, described here is another example of a secondary phosphate obtained from hand specimens in the Keck collection. The name and data for flurlite have been approved the International Mineralogical Association Commission on New Minerals, Nomenclature and Classification (IMA 2014–064). The mineral is named for Mathias von Flurl (1756–1823). He was the founder of mineralogy and geology studies in Bavaria and wrote the first book concerning these fields in Bavaria. He also produced the first geological map of Bavaria. The holotype specimen used for all the measurements is housed in the mineralogical collections of Museum Victoria, Melbourne, Victoria, Australia, registration number M53238.

Occurrence, mineral assemblage and paragenesis

Flurlite was found by one of the authors (EK) in the late 1970s in the Cornelia mine open cut of the Hagendorf-Süd pegmatite, Hagendorf, Oberpfalz, Bavaria, Germany (49°39′1″N 12°27′35″E). It is a very rare mineral that has been located in only a few specimens from the 67 m level of the mine. The red crystals labeled ‘oxidierter Schoonerit’ in figure 111 of Kastning and Schlüter (1994) are probably flurlite. The mineral occurs on green mitridatite and is associated closely with plimerite. Other associated minerals are beraunite, schoonerite, parascholzite/scholzite, robertsite and, occasionally, altered phosphophyllite.

Flurlite is a secondary phosphate mineral that has probably been formed from the hydrothermal reaction of zinc-bearing fluids or sphalerite with phosphate(s) derived from primary Fe-Mn phosphate minerals like triphylite or zwieselite. The paragenesis of the secondary phosphates at Hagendorf-Süd has been discussed in detail by Mücke (1981).

Physical and optical properties

At low magnification, flurlite appears as idiomorphic, blocky crystals with dimensions typically 50 μm to 100 μm, distributed on mounds of plimerite needles. At higher magnification grains are seen to be composed of very thin (<1 μm thick) platelets, shown edge-on in Fig. 1. The stacking of the platelets is splayed, giving characteristic twisted, accordion-like aggregates as shown in Fig. 2. The colour of the platelets ranges from a bright orange-red to a dark maroon-red (Fig. 3). The crystals are brittle, have a pearly lustre and are translucent when very thin. The streak is buff. Cleavage is excellent parallel to the dominant face of the platelets (001). No parting was observed and the fracture is irregular. The crystals were observed to float on diiodomethane (density = 3.32 g cm^{-3}) and remain suspended in bromoform (2.89 g cm^{-3}). The calculated density is 2.84 g cm^{-3} using the empirical formula.

Flurlite is biaxial (–) with measured refractive indices $\alpha = 1.60(1)$, $\beta = 1.65(1)$, $\gamma = 1.68(1)$ (white light). The 2V could not be measured; $2V_{calc} = 74°$. The crystals show weak dispersion and parallel extinction, with orientation: $X \approx c$, $Y \approx a$, $Z \approx b$. Pleochroism is weak, with colours: X = pale yellow, Y = pale orange, Z = orange brown. The Gladstone-Dale compatibility index (Mandarino, 1981)

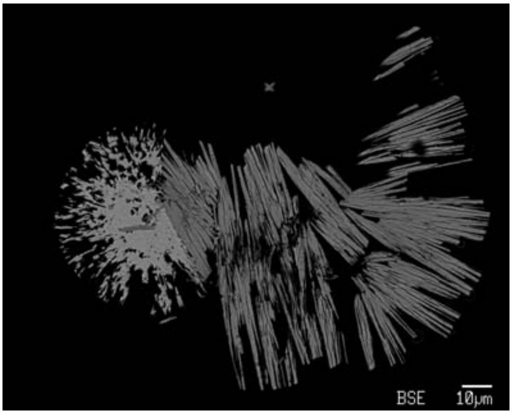

FIG. 1. Backscattered electron image of flurlite platelets viewed edge-on in the polished section used for the EMP analyses. The attached white mineral is plimerite.

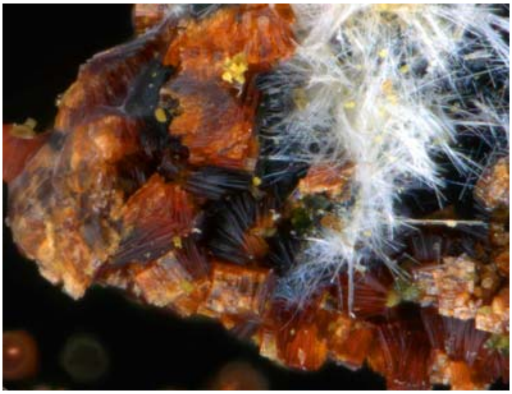

FIG. 3. Optical image of orange to dark red flurlite crystals. The white needles are plimerite.

calculated using the empirical formula is 0.006, which is classed as superior.

Chemical composition

Electron microprobe (EMP) analyses on crystals of flurlite were conducted using wavelength-dispersive spectrometry on a JEOL JXA 8500F Hyperprobe operated at an accelerating voltage of 12 kV and a beam current of 1 nA. The beam was defocused to 5 µm. Standards used were $AlPO_4$ for P, $MgAl_2O_4$ for Mg, hematite for Fe, $MnSiO_3$ for Mn, and ZnS for Zn. Water could not be analysed directly because of the minute amount of sample available. H_2O was calculated on the basis of 20 H atoms per formula unit (a.p.f.u.), in line with the crystal structure. The EMP results from the analysis of seven crystals (seven analyses) are given in Table 1. Despite the use of a defocused beam and low current, variable totals were obtained due to beam damage (water loss) and the very thin nature of the crystals, resulting in them being punctured by the beam.

The empirical formula (based on 3 P a.p.f.u.) with rounding errors is $(Zn_{2.5}Mn^{2+}_{0.6}Fe^{2+}_{0.8}Mg_{0.1})_{\Sigma 4.0}Fe^{3+}(PO_4)_3(OH)_2{\cdot}9H_2O$. The structural formula is $Zn(Mn_{0.6}Zn_{0.4})(Zn_{1.1}Fe_{0.8}Mg_{0.1})Fe^{3+}(PO_4)_3(OH)_2(H_2O)_7{\cdot}2H_2O$, showing seven cation-coordinated

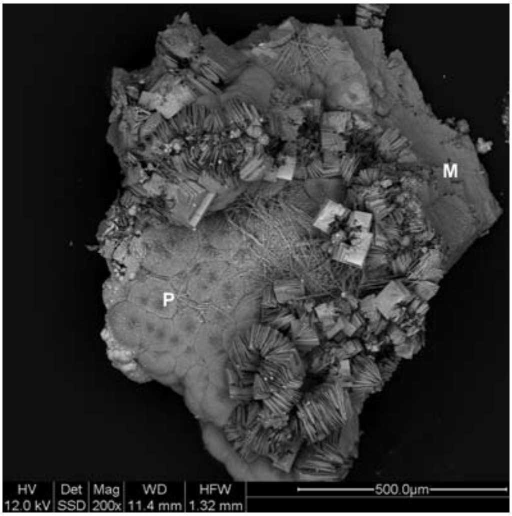

FIG. 2. Twisted aggregates of flurlite platelets. P = plimerite (refers also to the needles) and M = mitridatite.

TABLE 1. Analytical data for flurlite.

Constituent	wt.%	Range	SD
ZnO	25.40	23.4–27.2	1.2
MnO	5.28	4.26–7.23	0.95
MgO	0.52	0.25–0.63	0.12
Fe_2O_3*	10.30		
FeO*	7.40		
P_2O_5	27.20	25.6–28.3	0.9
H_2O**	23.10		
Total	99.20		

SD – standard deviation.
*Calculated from total Fe as Fe_2O_3 of 18.50 wt.%, range 15.8–24.0, SD 2.7, on the basis of 1 Fe^{3+} p.f.u.
**H_2O calculated on the basis of 20 H a.p.f.u.

water molecules and two interlayer water molecules p.f.u. The simplified formula is $Zn_3Mn^{2+}Fe^{3+}(PO_4)_3(OH)_2{\cdot}9H_2O$, based on dominant cations at each site in the structure.

Crystallography and structure refinement

Powder X-ray diffraction

The powder X-ray diffraction (XRD) pattern for flurlite is similar to the reported pattern for orthorhombic schoonerite, $ZnMn^{2+}Fe^{2+}_2Fe^{3+}(PO_4)_3(OH)_2{\cdot}9H_2O$ (Moore and Kampf, 1977) but with significant shifts in the positions of some reflections. The flurlite pattern was fitted by a lowering of the symmetry from orthorhombic to monoclinic. Powder XRD data were collected using a Philips diffractometer with graphite-monochromatized Co*K*α radiation. Data (in Å for Co*K*α) are reported in Table 2. Refinement of 28 2θ values using *CELLREF* (Laugier and Bochu, 2000) gave the following unit-cell parameters: $a = 6.392(3)$, $b = 11.047(2)$, $c = 13.067(3)$ Å, $\beta = 99.42(3)^{\circ}$, $V = 910.3(5)$ Å^3. The systematic absences were consistent with space group $P2_1/m$ (or $P2_1$, Pm), a maximal subgroup of the schoonerite space group *Pmab*.

TABLE 2. Powder diffraction data for flurlite.

I_{rel}	d_{meas}	d_{calc}	*h*	*k*	*l*
100	**12.900**	12.891	0	0	1
10	**8.375**	8.388	0	1	1
1	6.446	6.445	0	0	2
3	6.309	6.306	1	0	0
14	**6.072**	6.070	−1	0	1
8	**5.567**	5.567	0	1	2
2	5.473	5.476	1	1	0
3	5.325	5.320	−1	1	1
7	**5.080**	5.077	0	2	1
21	**4.297**	4.297	0	0	3
4	4.192	4.194	0	2	2
1	3.907	3.908	1	1	2
2	3.857	3.857	−1	0	3
2	3.641	3.641	−1	1	3
7	**3.221**	3.223	0	0	4
3	3.196	3.197	0	3	2
2	3.151	3.148	−1	3	1
2	3.095	3.094	0	1	4
1	2.967	2.968	−1	1	4
35	**2.763**	2.762	0	4	0
4	2.738	2.738	2	2	0
3	2.699	2.700	0	4	1
3	2.691	2.691	−1	2	4
1	2.336	2.336	0	2	5
4	2.149	2.148	0	0	6
2	2.103	2.104	−1	1	6
3	1.842	1.841	0	0	7
1	1.770	1.770	0	6	2

The strongest lines are given in bold.

Single-crystal studies

Crystals were examined initially using film methods. All crystals showed relatively severe streaking, consistent with the warping and splayed stacking of the platelets that is shown in Fig. 1. The streaking is illustrated in Fig. 4. A comparison of the (*hk*0) and (0*kl*) reciprocal lattice sections in Fig. 4 shows that the streaking is most pronounced parallel to **c***. An intensity data set was collected on one of the crystals using an Oxford Diffraction SuperNova diffractometer and Cu*K*α radiation.

The statistics of the normalized structure factors were consistent with the structure being centrosymmetric, space group $P2_1/m$. The structure was solved using the spin-flipping algorithm *Superflip*, implemented in *JANA2006* (Petříček and Dušek, 2006) and refined using *SHELXL* (Sheldrick, 2015). Although the refinement yielded sensible thermal parameters for all the atoms and calculated polyhedral bond lengths that were in the normal ranges for the metal atoms, the agreement factor R_1 could not be lowered below 0.16 for data to a resolution of 1 Å. The high agreement factor was considered to be due to the difficulty of obtaining a consistent integration of spot intensities in the data processing, due to the variable extent of streaking of the reflections as shown in Fig. 4.

Subsequently, beamtime was obtained at the microfocus beamline, MX2, at the Australian Synchrotron and intensity data were collected at 100 K on an ultrathin crystal for which the streaking was less severe. A structure solution was obtained using *SHELXT* (Sheldrick, 2015), which was found to be identical to that previously obtained with laboratory data except for an origin shift. Refinement using anisotropic displacement parameters for all atoms resulted in convergence at $R_1 = 0.057$ for 935 observed reflections to a resolution of 1 Å. An unambiguous location of H atoms in difference-Fourier maps could not be obtained. Details of the data collection and refinement are given in Table 3. The refined coordinates, equivalent isotropic displacement parameters and refined

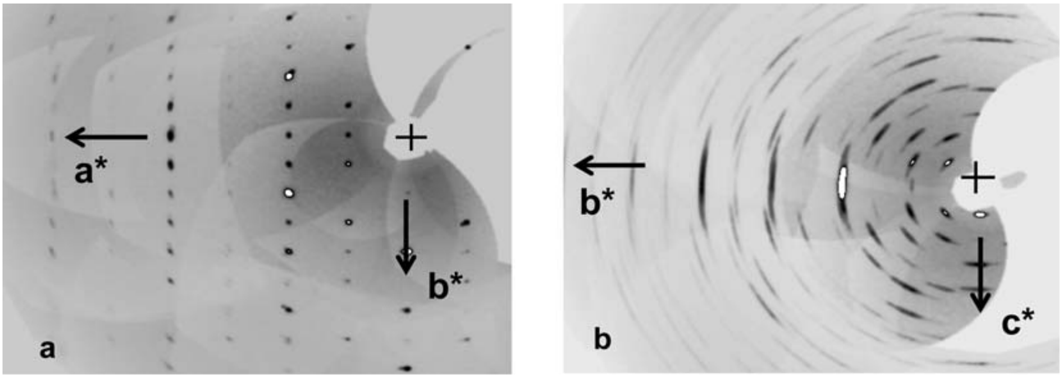

FIG. 4. XRD reciprocal lattice sections for a flurlite crystal. (*a*) *hk*0, (*b*) 0*k*l.

cation site occupancies are given in Table 4. Allocation of cations to the different sites was guided by a consideration of total electron scattering at the sites, bond valences, known common coordinations (e.g. predominatly Zn in the five-coordinated site) and site assignments in the related mineral schoonerite (Kampf, 1977). Tables of anisotropic displacement parameters and observed and calculated structure factors have been deposited with the Principal Editor of *Mineralogical Magazine* and are available from www.minersoc.org/pages/e_journals/dep_mat_mm.html.

TABLE 3. Crystal data and structure refinement for flurlite.

Empirical formula	$Zn_{2.5}Mn^{2+}_{0.6}Fe^{2+}_{0.8}Mg_{0.1}Fe^{3+}(PO_4)_3(OH)_2\cdot 9H_2O$
Formula weight	722.40
Temperature	100 K
Wavelength	0.71073 Å
Crystal system	Monoclinic
Space group	$P\,2_1/m$
Unit-cell parameters (100 K)	$a = 6.3710(13)$ Å $b = 11.020(2)$ Å $c = 13.016(3)$ Å $\beta = 99.34(3)°$
Volume	901.7(3) $Å^3$
Z	2
Density (calc., empirical formula)	2.84 g cm^{-3}
Absorption coefficient	4.661 mm^{-1}
Crystal size	0.02 × 0.02 × 0.003 mm^3
Theta range for data collection	2.4 to 20.8°
Index ranges	$-6 \le h \le 6$, $-11 \le k \le 11$, $-13 \le l \le 13$
Reflections collected	6570
Independent reflections	995 [$R_{int} = 0.0433$]
Completeness to $\theta = 20.8°$	98.7%
Refinement method	Full-matrix least-squares on F^2
Data / restraints / parameters	995 / 0 / 161
Goodness-of-fit on F^2	1.245
Final *R* indices [$F > 4\sigma(F)$]	$R_1 = 0.0566$, w$R_2 = 0.1486$
R indices (all data)	$R_1 = 0.0594$, w$R_2 = 0.1506$
Extinction coefficient	0.012(2)
Largest diff. peak and hole	1.265 and –0.750 e.$Å^{-3}$

TABLE 4. Atomic coordinates (×10^4), equivalent isotropic displacement parameters (Å^2 × 10^3) and calculated bond-valence (BV) sums for flurlite.

Atom	Site occupancy	*x*	*y*	*Z*	U_{eq}	BV
Zn1	0.76(8)Zn + 0.24(8)Fe	5853(4)	7500	7916(2)	20(1)	2.15
Zn2	0.54(6)Zn + 0.36(6)Fe + 0.1Mg	2477(3)	5001(2)	5090(2)	19(1)	2.02
Mn	0.52(6)Mn + 0.48(6)Zn	2190(4)	2500	8328(2)	19(2)	2.28
Fe	Fe	453(4)	7500	6275(2)	18(1)	3.12
P1		2772(6)	5301(3)	7650(3)	19(1)	4.99
P2		5296(8)	7500	5674(4)	17(2)	4.97
O1		2110(14)	4318(9)	8361(7)	21(2)	1.76
O2		3323(14)	4750(8)	6644(7)	20(2)	1.68
O3		900(14)	6187(8)	7360(7)	19(2)	1.74
O4		4758(14)	5947(9)	8226(7)	24(3)	1.82
O5		3570(20)	7500	6367(11)	23(4)	2.09
O6		7380(20)	7500	6473(11)	22(4)	1.94
O7		5114(15)	6333(8)	5024(8)	22(2)	1.80
OH		52(15)	6236(8)	5156(7)	21(2)	1.26
OW1		2286(15)	5269(9)	3441(8)	24(3)	0.31
OW2		4430(20)	2500	9729(11)	26(4)	0.36
OW3		–340(20)	2500	9220(11)	24(3)	0.36
OW4		4600(20)	2500	7336(11)	23(3)	0.33
OW5		–280(20)	2500	6889(10)	23(3)	0.26
OW6		8720(20)	7500	8746(12)	42(4)	0.50
OW7		7247(16)	4450(9)	9632(7)	27(3)	0

Description of the structure

The structure of flurlite is shown in projection along [100] in Fig. 5 and along [010] in Fig. 6*a*. It is a heteropolyhedral layer structure, with layers parallel to (001) and water molecules, Ow7, located between the layers. The slab-like layers contain two types of polyhedral chains running parallel to [100]

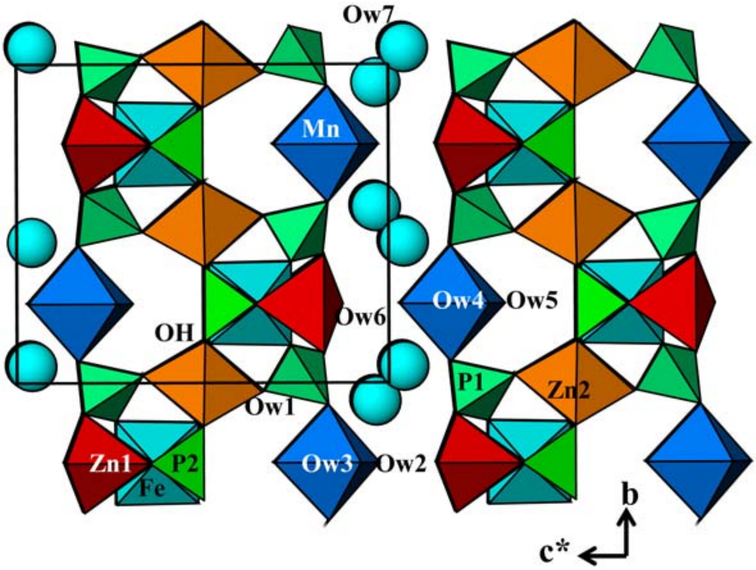

FIG. 5. The flurlite structure viewed along [100].

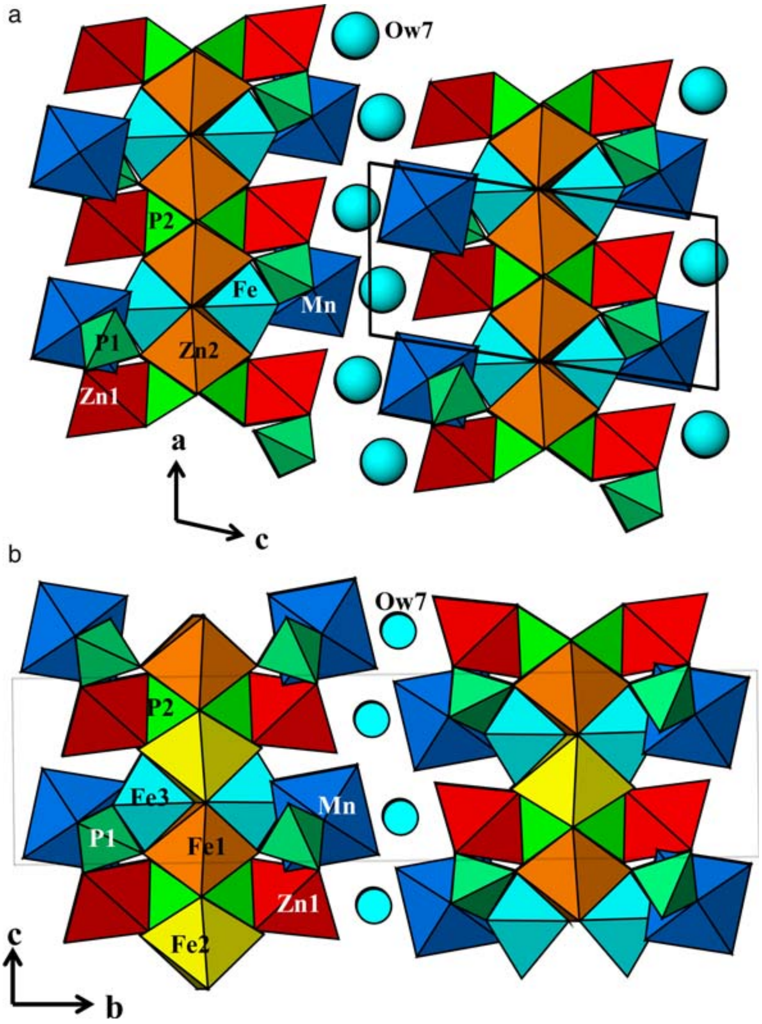

FIG. 6. (*a*) The flurlite structure viewed along [010]. (*b*) The schoonerite structure viewed along its 11 Å axis.

as shown in Fig. 6*a*. They are chains of edge-sharing Zn2-centred octahedra and chains of Fe^{3+}-centred octahedra that share their apices along [100] with dimers. The dimers comprise Zn1-centred trigonal bipyramids that share an edge with P2-centred tetrahedra. The two types of chains are corner-connected along [010]. The P1-centred tetrahedra connect the chains to $MnO_2(H_2O)_4$ octahedra along [010] to complete the structure of the (001) slabs.

Although the H atoms were not located, the assignment of water molecules and hydroxyl ions is straightforward based on bond valences. The results of the bond-valence calculations obtained using the program *BVCalc* in *WinGX* (Farrugia, 2012) are reported in Table 4. There is one hydroxyl anion, shared between Zn2 and Fe^{3+}-centred octahedra, and seven independent water molecules. The molecule Ow1 coordinates with Zn2, Ow2–5 coordinate with Mn and Ow6 coordinates with Zn1. The molecule Ow7 occupies the interlayer region, as shown in Fig. 6*a*. Hydrogen bonding involving Ow7 is responsible for binding adjacent layers. As listed in Table 5, Ow7 acts as a donor of H bonds to O1 and O4, and as an acceptor for bonds from Ow2 and Ow3. Hydrogen bonds involving the water molecules and the hydroxyl ion are listed in Table 5.

TABLE 5. Polyhedral bond distances and hydrogen bonds (Å) for flurlite.

Zn1–O4 (×2)	1.915(10)	P1–O1	1.527(10)
–OW6	1.967(15)	–O2	1.535(10)
–O6	2.253(13)	–O3	1.537(10)
–O5	2.286(14)	–O4	1.540(10)
mean	2.067	mean	1.535
Zn2–O2	2.026(10)	P2–O5	1.530(15)
–OH	2.072(9)	–O7 (×2)	1.534(10)
–OH	2.095(9)	–O6	1.549(14)
–O7	2.147(9)	mean	1.537
–OW1	2.150(10)		
–O7	2.243(10)	H bonds	
mean	2.122	OH···OW5	3.03(2)
		OW1···O3	2.66(1)
Mn–O1 (×2)	2.005(10)	OW2···OW7	2.81(1)
–OW2	2.125(14)	OW3···OW7	2.74(1)
–OW3	2.136(14)	OW4···O2	2.72(1)
–OW4	2.158(13)	OW5···OW1	2.77(1)
–OW5	2.242(13)	OW6···O3	2.84(1)
mean	2.112	OW6···OW3	2.68(2)
		OW7···O1	2.91(1)
Fe–O5	1.971(13)	OW7···O4	2.78(1)
–OH (×2)	2.001(9)		
–O3 (×2)	2.010(9)		
–O6	2.014(13)		
mean	2.001		

Cation distributions in the metal atom sites, obtained from site-occupancy refinements are reported in Table 4. The sites Zn1, Zn2 and Mn involved refinement of the relative amounts of Zn/Fe, Zn/Fe and Mn/Zn respectively. The minor amount of Mg was incorporated in site Zn2 and not refined. Site Fe was fully occupied by iron and bond-valence calculations showed that it was in the ferric state, as also found for schoonerite (Kampf, 1977), whereas the other sites contain only divalent cations. The composition obtained from the site refinements is $(Zn_{2.3}Mn^{2+}{}_{0.5}Fe^{2+}{}_{1.0}Mg_{0.2})_{\Sigma 4.0}Fe^{3+}(PO_4)_3(OH)_2{\cdot}9H_2O$, in good agreement with the empirical formula from the EMP analyses, $(Zn_{2.5}Mn^{2+}{}_{0.6}Fe^{2+}{}_{0.8}Mg_{0.1})_{\Sigma 4.0}Fe^{3+}(PO_4)_3(OH)_2{\cdot}9H_2O$.

Flurlite is related chemically and structurally to schoonerite (Moore and Kampf, 1977; Kampf, 1977). The similarities and differences between the two minerals are indicated by comparative data in Table 6. Flurlite has the same stoichiometry as schoonerite but differs in having dominant Zn in the 6.4 Å edge-shared octahedral chains, whereas schoonerite has dominant ferrous iron in these sites. The structure of falsterite, $Ca_2MgMn_2^{2+}(Fe_{0.5}^{2+}Fe_{0.5}^{3+})_4Zn_4(PO_4)_8(OH)_4(H_2O)_{14}$, also contains edge-shared octahedral chains with a 6.4 Å repeat (Kampf *et al.*, 2012). The structural relationships between schoonerite and falsterite have been discussed by Kampf *et al.* (2012).

Both flurlite and schoonerite have layer structures with water molecules between the layers and with similar repeat distances in the layers (~6.4 Å × 11.1 Å). However, schoonerite is orthorhombic, *Pmab*, while flurlite is monoclinic, $P2_1/m$, and the different symmetry elements within the layers in the two structures results in different topologies. This is illustrated in Fig. 7, where the different linkings of the P1-centred tetrahedra to the octahedra in the 6.4 Å chains in both structures are

TABLE 6. Comparative data for schoonerite and flurlite.

	Schoonerite	Flurlite
Formula	$ZnMnFe_2^{2+}Fe^{3+}(PO_4)_3(OH)_2{\cdot}9H_2O$	$Zn_3MnFe^{3+}(PO_4)_3(OH)_2{\cdot}9H_2O$
Symmetry	Orthorhombic, *Pmab*	Monoclinic, $P2_1/m$
Cell	$a = 11.119(4)$, $b = 25.546(11)$, $c = 6.437(3)$ Å	$a = 6.371(1)$, $b = 11.020(2)$, $c = 13.016(3)$ Å, $\beta = 99.34(3)°$
Z	4	2
Strongest powder pattern lines *d, I, hkl*	12.77, 100, (020)	12.900, 100, (001)
	8.33, 70, (120)	8.375, 10, (011)
	6.43, 40, (001)	6.072, 14, ($\bar{1}01$)
	3.761, 40, (151)	5.567, 8, (012)
	3.182, 40, (311)	4.297, 21, (003)
	2.768, 90, (400)	2.763, 35, (040)
Optics	Biaxial (–). $\alpha = 1.618(5)$, $\beta = 1.652(3)$, $\gamma = 1.682(3)$	Biaxial (–). $\alpha = 1.60(1)$, $\beta = 1.65(1)$, $\gamma = 1.68(1)$

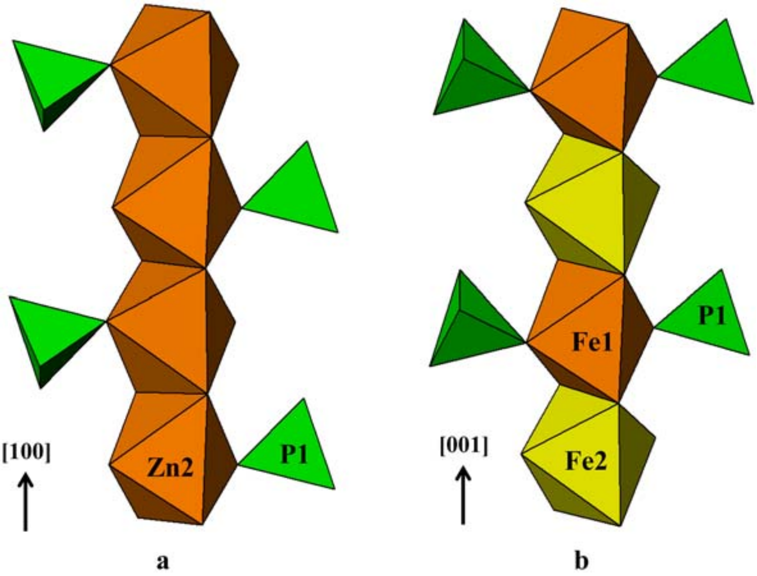

FIG. 7. Coordination of P1-centred tetrahedra to 6.4 Å octahedral chains in (*a*) flurlite and (*b*) schoonerite.

compared. In flurlite the Zn2-centred octahedra forming the edge-shared chains have the composition $ZnO_3(OH)_2H_2O$ whereas in schoonerite two types of octahedra alternate along the chains, with compositions $FeO_4(OH)_2$ and $FeO_2(OH)_2(H_2O)_2$. The two structures have different orientation relationships between symmetry-related sites on opposite sides of the slabs as seen by a comparison of the 11.1 Å projections for flurlite in Fig. 6*a* and schoonerite in Fig. 6*b*. These Figures show that a twinning relationship exists between the two structures. The schoonerite structure can be derived from that of flurlite by rotation of the atoms in one half of the (001) slabs about a two-fold axis parallel to [100] and passing through the chains of edge-shared octahedra. It is expected that intergrowth of twinned and untwinned elements should occur readily. Disordered mixing of the two types of layers could contribute to the severe streaking observed in the diffraction patterns.

Acknowledgements

Diffraction data used in the flurlite structure analysis were collected at the macromolecular microfocus beamline MX2 at the Australian Synchrotron, Victoria and at Melbourne University, School of Chemistry. Cameron Davidson is thanked for sample preparation for the EMP studies.

References

Bernard, J.H. and Hyršl, J. (2004) *Minerals and their localities* (V.T. King, editor). Granit, Prague, Czech Republic.

Birch, W.D., Grey, I.E., Mills, S.J., Pring, A. Wilson, N.C. and Keck, E. (2011) Nordgauite, $MnAl_2(PO_4)_2(F,OH)_2\cdot 5H_2O$, a new mineral from the Hagendorf Süd pegmatite, Bavaria, Germany: description and crystal structure. *Mineralogical Magazine*, **75**, 269–278.

Farrugia, L.J. (2012) WinGX and ORTEP for Windows: an update. *Journal of Applied Crystallography*, **45**, 849–854.

Frondel, C. (1958) Strunzite, a new mineral. *Naturwissenschaften*, **45**, 37.

Kampf, A.R. (1977) Schoonerite: its atomic arrangement. *American Mineralogist*, **62**, 250–255.

Kampf, A.R., Mills, S.J., Simmons, W.B., Nizamoff, J.W. and Whitmore, R.W. (2012) Falsterite, $Ca_2MgMn_2^{2+}(Fe_{0.5}^{2+}Fe_{0.5}^{3+})_4Zn_4(PO_4)_8(OH)_4(H_2O)_{14}$, a new secondary phosphate mineral from the Palermo No. 1 pegmatite, North Groton, New Hampshire. *American Mineralogist*, **97**, 496–502.

Kastning, J. and Schlüter, J. (1994) *Die Mineralien von Hagendorf und ihre Bestimmung. Schriften des Mineralogischen Museums der Universitat Hamburf*, Band 2, C. Weise Verlag, Munich, 95 pp.

Laubmann, H. and Steinmetz, H. (1920) Phosphatführende pegmatite des Oberfalzer und Bayerischen Waldes. *Zeitschrift für Krystallografie und Mineralogie*, **55**, 523–586.

Laugier, J. and Bochu, B. (2000) *LMGP-Program for the interpretation of X-ray experiments*. INPG/Laboratoire des Matériaux et du Génie Physique, St Martin d'Heres, France.

Mandarino, J.A. (1981) The Gladstone-Dale relationship: Part IV. The compatibility concept and its application. *The Canadian Mineralogist*, **19**, 441–450.

Moore, P.B. and Kampf, A.R. (1977) Schoonerite, a new zinc-manganese-iron phosphate mineral. *American Mineralogist*, **62**, 246–249.

Mücke, A. (1981) The paragenesis of the phosphate minerals of the Hagendorf pegmatite – a general view. *Chemie der Erde*, **40**, 217–234.

Müllbauer, F. (1925) Die Phosphatpegmatite von Hagendorf i. Bayern (neue Beobachtungen). *Zeitschrift für Krystallographie*, **61**, 331–336.

Petříček, V. and Dušek, M. (2006) *JANA2006. Structure Determinations Software Programs*. Institute of Physics, Academy of Sciences of the Czech Republic, Prague.

Sheldrick, G.M. (2015) Crystal structure refinement with *SHELXL*. *Acta Crystallographica*, **C71**, 3–8.

Strunz, H. (1950) Scholzit, eine neue Mineralart. *Fortschritte der Mineralogie*, **27**, 31.

Strunz, H. (1954*a*) Hagendorfit, ein neues Mineral der Varulith-Hühnerkobelit-Reihe. *Neues Jahrbuch für Mineralogie Monatshafte*, 252–255.

Strunz, H. (1954*b*) Laueit, $MnFe_2III(PO_4)_2(OH)_2 \cdot 8H_2O$, ein neues Mineral. *Naturwissenschaften*, **41**, 256.

Strunz, H. (1956) Pseudolaueit, ein neues Mineral. *Naturwissenschaften*, **43**, 128.

Yakovenchuk, V.N., Keck, E., Krivovichev, S.V., Pakhomovsky, Y.A., Selivanova, E.A., Mikhailova, J.A., Chernyatieva, A.P. and Ivanyuk, G.Yu. (2012) Whiteite-(CaMnMn), $CaMnMn_2Al_2[PO_4]_4(OH)_2 \cdot 8H_2O$, a new mineral from the Hagendorf-Süd granitic pegmatite, Germany. *Mineralogical Magazine*, **76**, 2761–2771.